Voltage-gated sodium channels support action potential propagation in prefrontal basal dendrites: direct evidence from local TTX application

In basal dendrites of somatosensory cortex, blocking sodium channels was shown to have no effect on calcium influx in distal basal dendrites following single backpropagating action potentials (bAPs) (Kampa and Stuart 2006), suggesting that the bAPs themselves are unaffected by sodium channel block.

Here we use voltage imaging and analyze the contribution of sodium channels to single bAPs in basal dendrites of prefrontal cortical pyramidal cells by locally applying TTX. Following control measurements in normal ACSF (Suppl. Fig. S1C, Control), 7 MΩ glass pipettes filled with 5 μM TTX positioned near (~20μm) the mid regions of individual basal dendrites (Fig. S1B) were used to focally apply TTX using brief pulses of pressure (duration = 1 sec). Pressure pulses were stopped 1 sec before opening the shutter that controls epi-illumination light. TTX pipettes were positioned away from the soma such that the somatic action potential amplitudes were not affected by TTX application (TTX/Control = 98 ± 3.8 %, n = 5). Notable reductions in AP peak amplitudes were observed when dendritic action potentials were re-recorded optically, immediately following TTX application pulses (Suppl. Fig. S1C, TTX). Neuron position and focus were kept fixed between subsequent recordings allowing relative comparisons of signals sampled from the same dendritic segment in two subsequent recording sweeps (Milojkovic et al. 2004; Djurisic et al. 2004). The effect of TTX was reversible after a 5 minute washout period (Fig. S1C, Washout) confirming the stability of recordings, and that observed effects were due to the actions of TTX and not damage to dendrites. Reduction in amplitude at, and distal to, the TTX application pipette was similar in 5 cells examined (data not shown).

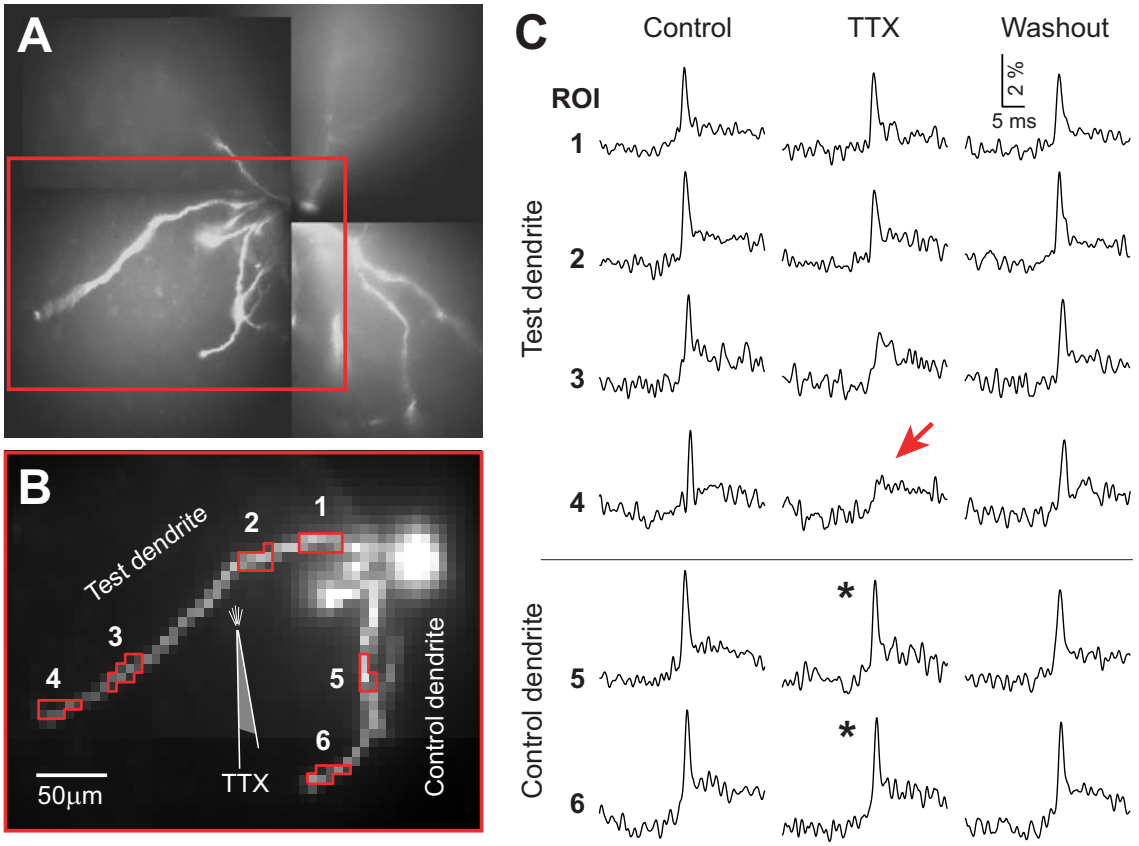

Suppl. Fig. S1. Local TTX application reveals the importance of sodium channels in action potential backpropagation in basal dendrites of layer V pyramidal neurons in the rat prefrontal cortex.

(**A**) Composite microphotograph (40X magnification objective) of a layer V pyramidal cell filled with fluorescent voltage-sensitive dye JPW1114. The lipophilic dye JPW1114 was delivered into the cell body via diffusion from the whole-cell pipette. Next, the dye-loading pipette was pulled out and the brain slice was incubated for approximately one hour at room temperature. Prior to optical recording the neuron was re-patched with dye-free pipette. Box indicates region of optical recording shown in panel **B**. Apical dendrite is oriented vertically and is obscured by patch pipette. (**B**) One frame (containing selected basal dendrites) was acquired with fast data acquisition CCD at 2000 Hz full-frame rate. At this magnification (40X objective lens) each pixel captures 6.1 x 6.1 μm in the object field. Local TTX application pipette placement is indicated by the drawing. Detector sets (pixel sets) outlined correspond to six regions of interest (ROIs), four on the test dendrite near the TTX pipette, two on the control dendrite – away from the TTX pipette. (**C**) Action potentials were evoked by somatic current pulse stimulation. Action potentials associated optical signals were sampled from multiple sites before TTX application (Control), right after TTX pressure application (TTX), and 5 min after the cessation of a TTX pulse (Washout). Five minute washout was chosen conservatively to reduce the risk from JPW1114 phototoxicity (Antic et al. 1999). Each trace is a product of spike-triggered averaging (N = 5 sweeps). Action potential amplitude is severely reduced in the tip of the Test dendrite (ROI 4, red arrow), but not in the Control dendrite (ROIs 5 and 6). Somatic action potential amplitude obtained in whole-cell recording is unaffected by focal TTX application (not shown).

Effect of I_h on subthreshold membrane properties and action potential backpropagation in prefrontal cortical basal dendrites

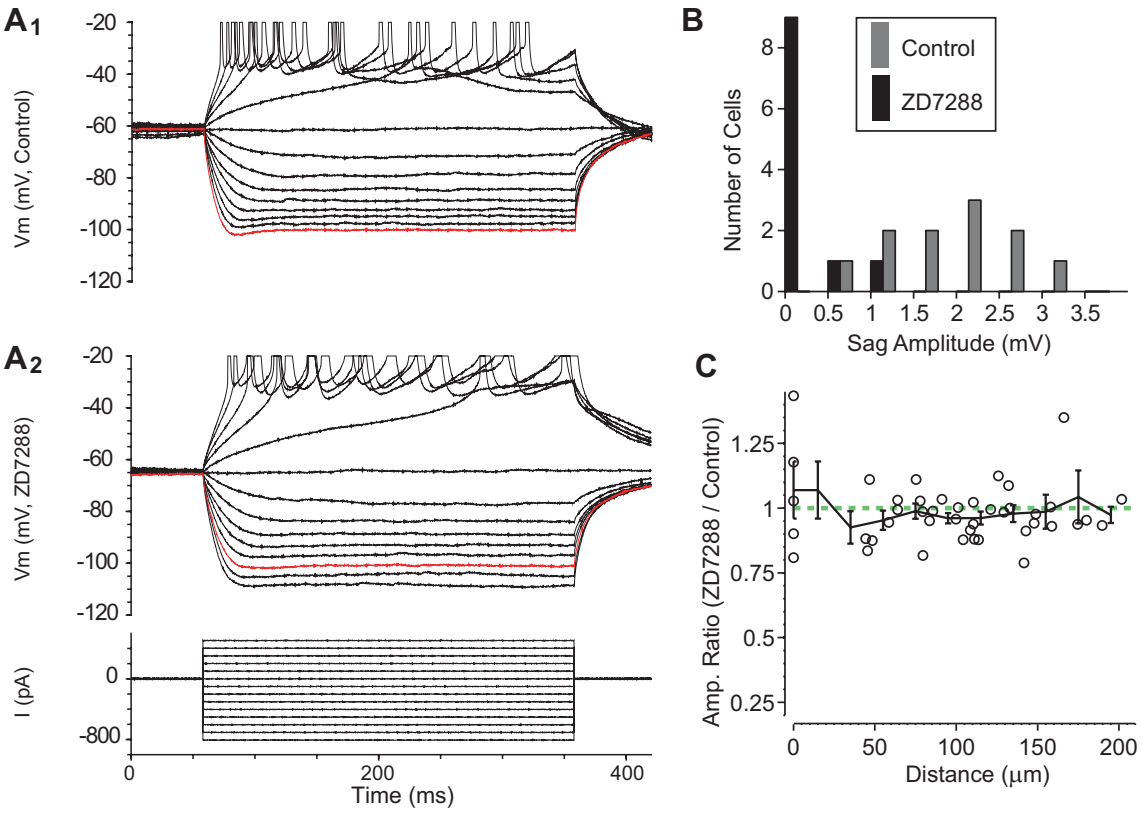

Suppl. Fig. S2. I_h has little or no effect on action potential backpropagation in basal dendrites of layer V prefrontal pyramidal neurons. Before the actual voltage-sensitive dye recordings were made we performed electrophysiological measurements to determine the potency of our batch of ZD7288 to block the hyperpolarization-evoked sag in somatic whole-cell recordings. (**A1**) In normal ACSF hyperpolarizing current pulses (bottom inset) produced small 1-3 mV sag (red sweep). (**A2**) Bath application of I_h channel blocker ZD7288 (20 μM) extinguished the sag. (**B**) Summary data of sag amplitudes measured near -100 mV in control and ZD7288 conditions (N = 28 neurons). (**C**) Amplitude ratios of backpropagating action potentials recorded optically along basal dendrites, ZD7288 conditions over Control, as a function of distance from soma. N = 10 dendritic branches from 5 neurons. Error bars = sem. Green dashed line marks the ratio of 1 (e.g. no difference between Control and ZD7288 condition).

Contribution of delayed rectifier potassium channels to action potential backpropagation in basal dendrites

In order to determine the effect of delayed rectifier potassium channels on action potential backpropagation in prefrontal cortical basal dendrites, we performed voltage-sensitive dye measurements before and after application of the pharmacological blocker TEA. First, we showed that TEA significantly increases action potential width. In 6 neurons recorded with no voltage-sensitive dye applied (electrophysiology only), the somatic AP half-widths were 1.6 $\pm$ 0.1 ms in 5 mM TEA compare to control measurement obtained in the same neuron prior to bath application of TEA (0.9 $\pm$ 0.1 ms) .

Optical recordings with voltage-sensitive dye showed a similar increase in somatic half width (Suppl. Fig. S3B), along with notable increase in AP widths at dendritic locations (Suppl. Fig. S3D). At the same time, TEA did not cause a significant increase in action potential amplitude in the basal dendrites tested (Suppl. Fig. 3C). TEA has been shown to block A-type potassium channels to a considerable degree along with delay rectifier channels in hippocampal pyramidal neurons (Hoffman et al. 1997). Given that 4-AP increased widths to a greater extent far from the soma (Fig. 3), results here are consistent with collateral blockage of A-type potassium channels (by TEA). Therefore, it is not possible to determine how much of the observed increased in amplitude in TEA can be ascribed to delayed rectifier potassium channels.

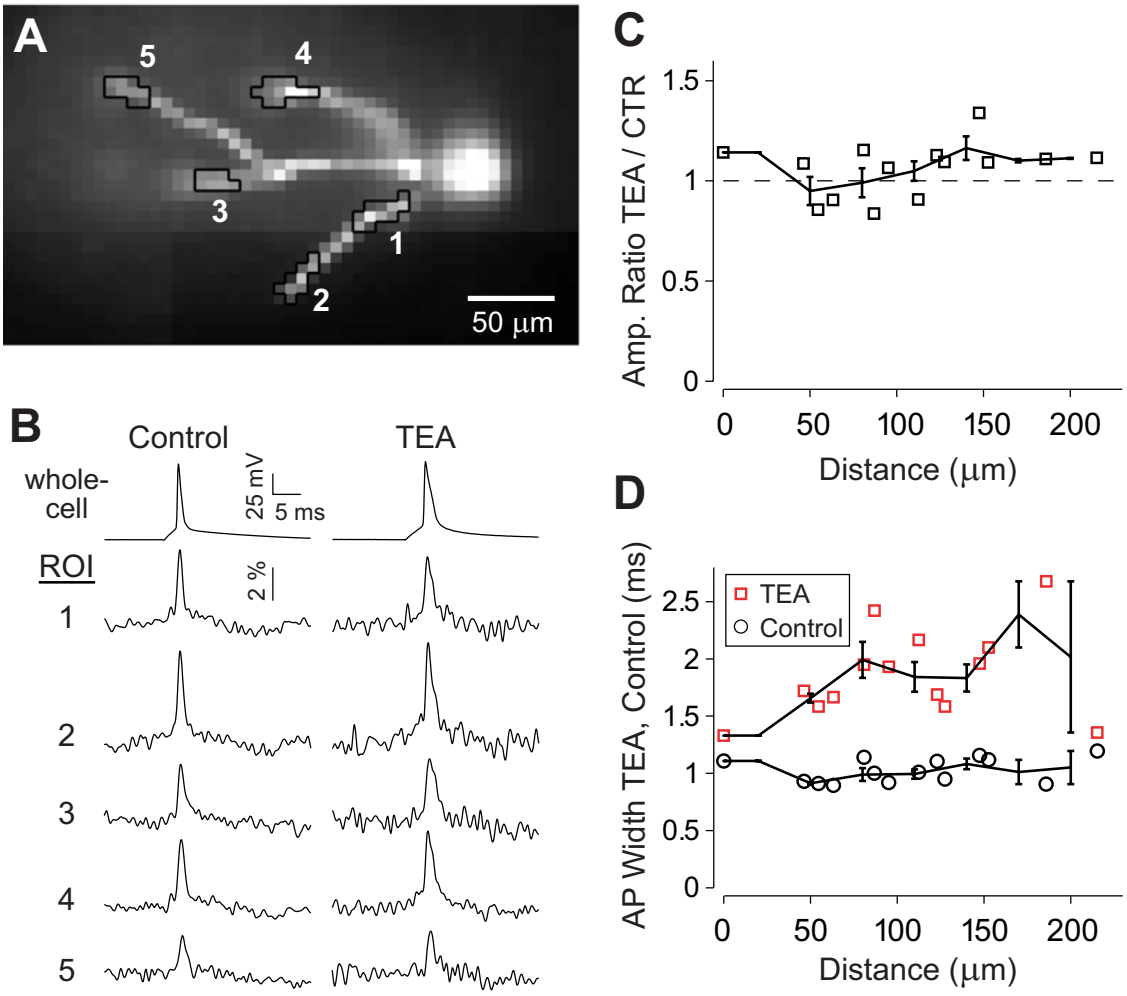

Suppl. Fig. S3. The effect of potassium channel blocker TEA (5 mM) on action potential backpropagation in prefrontal cortex.

(**A**) Layer 5 pyramidal neuron loaded with JPW3028 in the brain slice harvested from the rat prefrontal cortex. One NeuroCCD frame (2000 Hz frame rate) captures a section of the basal arbor. Five regions of interest (ROIs) are outlined. (**B**) Somatic whole-cell recordings of single action potentials are aligned with simultaneous optically recorded AP waveforms from regions of interest 1-5 outlined in ***A***. AP peak amplitudes were first recorded in normal ACSF (Control) and then TEA (5 mM) was introduced in the perfusion system and the simultaneous electrical and optical recordings were repeated on the same neuron (TEA). (**C**) Action potential amplitude ratios TEA/Control, as a function of distance from the soma for all branches. (**D**) Action potential widths as a function of distance for Control (black circles) and TEA (red squares) conditions.

AP amplitudes tend to be larger in shorter dendrites compared to longer ones in the present multi-compartmental model

When model AP amplitudes are plotted as a function of the distance from the soma in many basal branches (See Fig. 6B, thin grey lines), the longer branches seem to have smaller amplitudes overall in the present model. Two different dendritic regions, both situated at the same distance from the soma (150 µm), but on different basal dendrites with different lengths, exhibit a significant difference in action potential amplitude. For example, in the longer basal dendrite (dend. 1) the peak amplitude of the dendritic AP is 62 % of the somatic AP (Suppl. Fig. S4). While in the shorter dendrite (dend. 2), at the same distance (150 µm) from the soma, the peak amplitude of the dendritic AP is 74 % of the somatic AP (Suppl. Fig. S4).

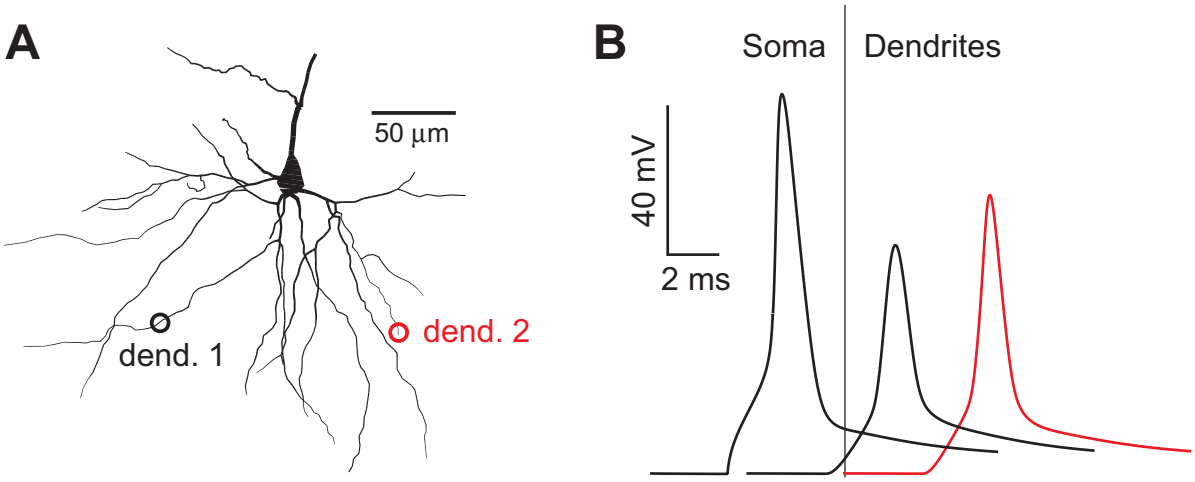

Suppl. Fig. S4. Significant difference in AP amplitudes in dendrites with different lengths in the present model of basal dendrites of layer V pyramidal neurons from rat prefrontal cortex. (**A**) Basal dendrites of reconstructed pyramidal neuron with two dendritic locations indicated by circles, both at 150 µm from the cell body. Same neuron as in Fig. 6A. (**B**) Side-by-side comparison of three action potential waveforms obtained simultaneously at three separate "recording" locations shown in ***A*** (soma; dend.1 – black; dend.2 – red). Amplitude of dendritic AP in "*dend. 1*" is 74% while in "*dend.2*" it is 62% of the somatic AP.

Analysis of action potential waveforms

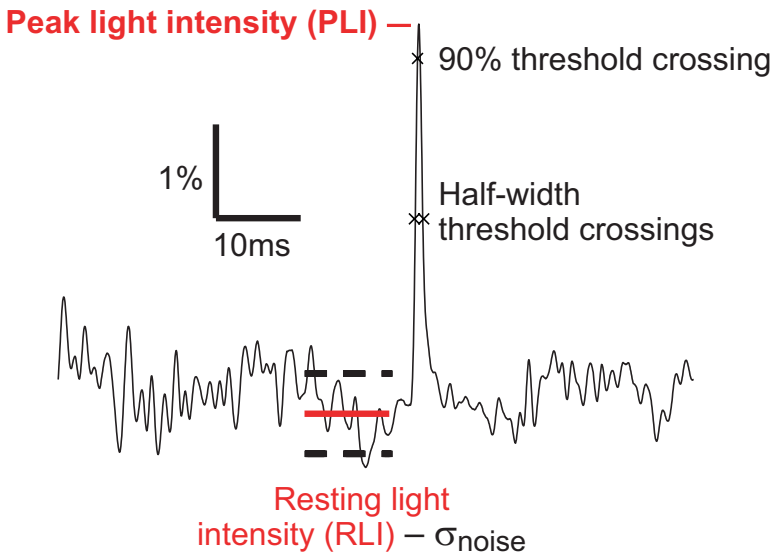

Suppl. Fig. S5. Analysis of APs obtained by voltage-sensitive dye imaging. Optical signal were analyzed using the custom made software (in MATLAB). Action potential amplitudes are computed by finding the peak (peak light intensity, PLI, red line at the top) and resting light intensity (RLI, red solid line at the bottom) from the fluorescence signal. RLI is the mean of a 10 ms window of data preceding the peak by 3.5 ms. Percent fluorescence signal, $\Delta F/F$, is calculated as: (PLI-RLI)/RLI*100. Standard deviation of noise is computed using the data preceding stimulus by more than 3.5 ms, after first high-pass filtering (3 dB cutoff at 45 Hz, Chebyshev Type II, 3rd order, σ_{noise}). Half width is determined half way between RLI and PLI using linear interpolation. 90 % threshold crossings are used for latency measurements.

Correction of underestimated dendritic lengths

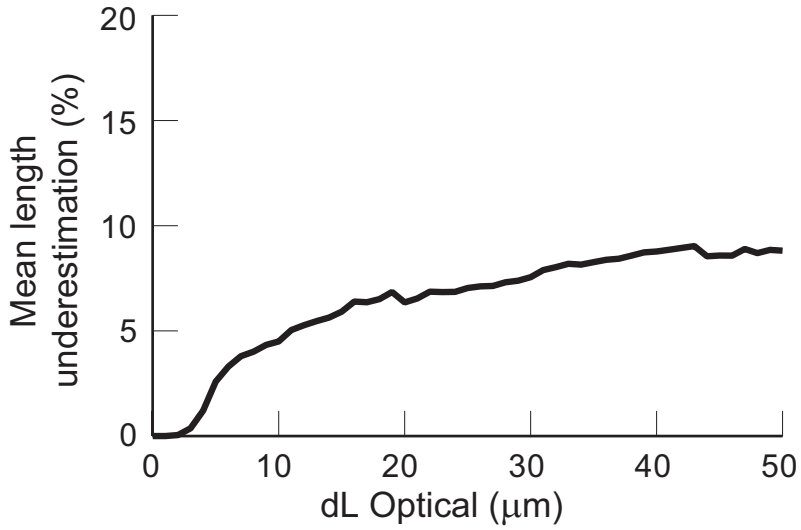

Suppl. Fig. S6. Correction of underestimated dendritic lengths.
Distances between ROIs were measured using 80 x 80 pixel images captured by fast NeuroCCD data acquisition camera. This creates an underestimation of dendritic lengths by approximately 7%. The graph represents mean length underestimation over all basal dendrites of a reconstructed prefrontal pyramidal neuron (shown Fig. 6A) as a function of the straight line distance between two points (dL Optical, corresponds to distance between ROI centers). For all pairs of points separated by the straight line distance of dL Optical, the true path length following the fine scale dendritic curvature is calculated (PL for path length). Underestimation: (PL-dL)/PL*100. For more details see Methods section.

What combinations of dendritic gNa and gKA would allow for significant branch strength potentiation (BSP)?

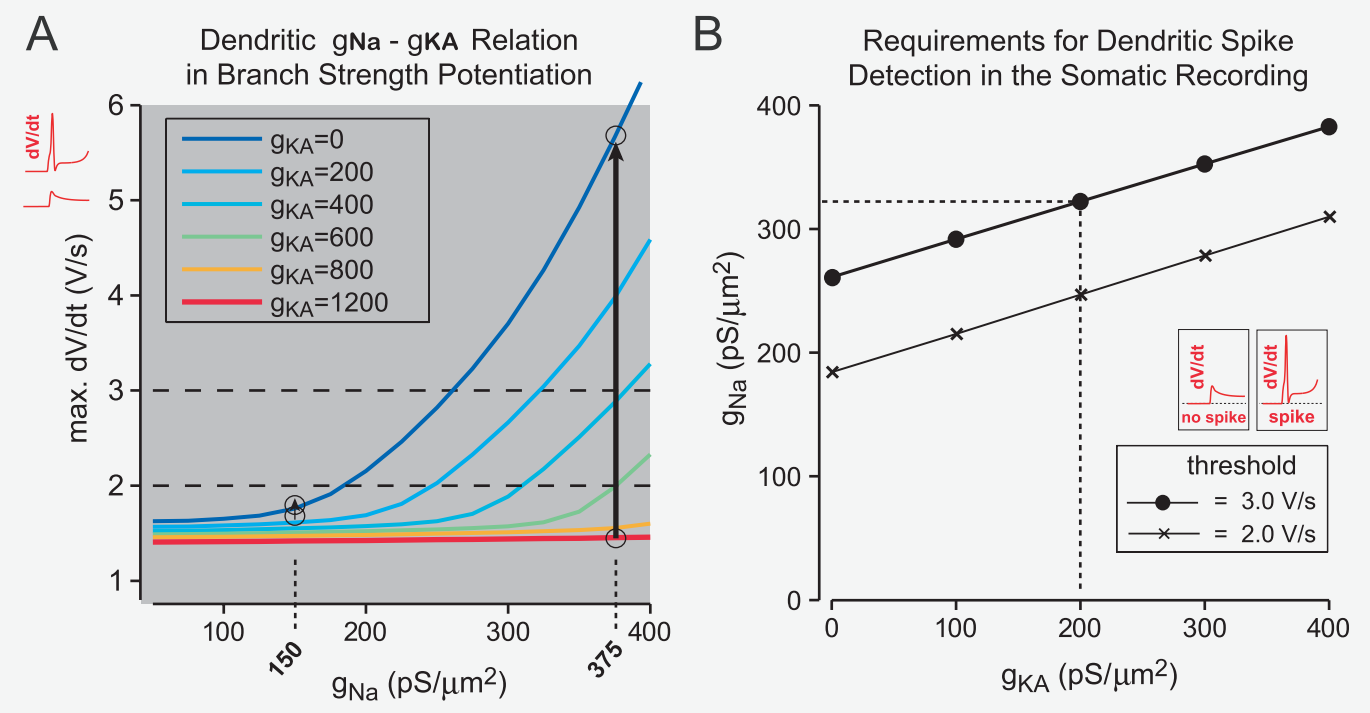

Suppl. Fig. S7. All simulations were performed using an identical plateau-conductance change delivered at the same location in distal dendritic segment shown in Fig. 10A, Inset. The only two parameters varied in this series of simulations were proximal g_{Na} and g_{KA} in the target dendrite. A decreasing slope for g_{Na} and increasing slope for g_{KA} with distance from soma were as described in best fit model. The peak of the first derivative of somatic membrane potential preceding the first action potential (see Fig. 10B, bottom trace, arrow) indicates the strength of the dendritic spike initiated by dendritic stimulation.

(**A**) Maximum values of the first derivative (dV/dt) of somatic voltage waveform is plotted as a function of the model's proximal basal dendritic sodium conductance g_{Na}, for several values of proximal basal dendritic A-type potassium conductance g_{KA} (g_{KA} values are color-coded). Vertical arrows show the effect of blocking I_A and the resulting increase in the somatic dV/dt response for normal (g_{Na}=150) and special case (g_{Na}=375 pS/µm^2) sodium distributions (as described in Fig. 10AB). Dashed lines are two arbitrary thresholds created to explain the numerical example in **B**. (**B**) If one were to use a simple threshold on somatic dV/dt to determine the presence of a local dendritic spike, one can determine the basal dendritic sodium and A-type potassium distributions required to meet this criterion. Plotted are the g_{Na} and g_{KA} values from panel *A* that cross the two hypothetical thresholds shown. Y-intercepts show the minimum values of g_{Na} necessary to generate a dendritic spike that leads to a super-threshold (arbitrary threshold on dV/dt, not spike threshold) response when g_{KA} is completely blocked (downregulated). Inverse slopes of both lines are ~3.2 meaning that I_{Na} has a greater influence in enhancing dendritic spikes compared to the inhibiting effect of I_A (by a factor near 3.2), and this is largely independent of the arbitrarily chosen threshold. Dashed lines represent an illustrative numerical example: If proximal g_{KA} were set at 200 pS/µm^2, then the minimal dendritic gNa required to produce significant conversion from WEAK to STRONG dendrite (upon I_A downregulation) must be greater than 320 pS/µm^2. In this numerical example dendrite is considered STRONG if dV/dt ≥ 3 V/s.

References

Antic S, Major G, and Zecevic D. Fast optical recordings of membrane potential changes from dendrites of pyramidal neurons. *J Neurophysiol* 82: 1615-1621, 1999.

Djurisic M, Antic S, Chen WR, and Zecevic D. Voltage imaging from dendrites of mitral cells: EPSP attenuation and spike trigger zones. *J Neurosci* 24: 6703-6714, 2004.

Hoffman DA, Magee JC, Colbert CM, and Johnston D. K+ channel regulation of signal propagation in dendrites of hippocampal pyramidal neurons. *Nature* 387: 869-875, 1997.

Kampa BM and Stuart GJ. Calcium spikes in basal dendrites of layer 5 pyramidal neurons during action potential bursts. *J Neurosci* 26: 7424-7432, 2006.

Milojkovic BA, Radojicic MS, Goldman-Rakic PS, and Antic SD. Burst generation in rat pyramidal neurones by regenerative potentials elicited in a restricted part of the basilar dendritic tree. *J Physiol* 558: 193-211, 2004.

*